International Journal of
INTELLIGENT SYSTEMS AND APPLICATIONS IN ENGINEERING
ISSN:2147-6799 www.ijisae.org Original Research Paper

Fully Conventional Generator Network for Colorectal Polyp Segmentation in Colonoscopy Images

M.N. Prashanth*[1], S. Senthilkumar[2]

Submitted: 29/01/2024 **Revised**: 07/03/2024 **Accepted**: 15/03/2024

Abstract: The early stage of Colorectal cancer (CRC) prediction is useful to decrease the mortality and morbidity rate and also to increase the diagnosis efficiency of the patient-specific treatments. CRCs are treatable if the polyps are detected in the earliest stages. Colonoscopy has established itself as a useful diagnostic method for examining abnormalities in the lower digestive system and can accurately localize lesions. We propose a novel segmentation network, Fully Convolutional Generator Network(FCG-Net), for automatic localization and segmentation of polyps using colonoscopy images. The generator model based on the fully convolutional network can realize the segmentation network's end-to-end output and enrich the semantic information of polyps through transverse connections. FCG-Net can also input the segmentation prediction images and the labeled images into the discriminant convolutional network and improve the segmentation accuracy of polyps by further enhancing the essential characteristics of learning data through the confrontation training of generators and discriminators. The experimental results demonstrate that higher performance is provided by the newly developed FCGN-Net predictive model when compared to other comparative algorithms while considering the negative and positive metrics.

Keywords: *Colonoscopy; Colorectal Cancer; CNN; Normal analysis.*

1. Introduction

Colorectal cancer (CRC), one of the ultimate stages of the GI tract polyp, is caused by the abnormal development or swelling of tissues in the GI tract. Currently, CRCs are treatable if the polyps are detected in the earliest stages. Colonoscopy has established itself as a useful diagnostic method for examining abnormalities in the lower digestive system and can accurately localize lesions. Traditional colonoscopy, however, is uncomfortable and intrusive and is ineffective for treating abnormalities in the small intestine. Lesion form, color, irregularity, size, and texture are only a few of the difficulties that are currently present in this field. Numerous computer-based strategies are used for polyp segmentation. CRC being the third most prevalent type of cancer in the world and having a high mortality rate, colorectal cancer (CRC) is one of the largest health problems[1]. The early stage of Colo-rectal cancer (CRC) prediction is useful to decrease the mortality and morbidity rate and also to increase the diagnosis efficiency of the patient-specific treatments. Existing CRC prediction approaches suffer from several limitations because of unreliable human false-positive predictive outcomes. The deep learning-based diagnosis methodology provides higher prediction accuracy and earlier detection of Polyps from the collected data set. But, the researchers face several challenges in the prediction of thyroid nodules from large dimensional dataset with higher prediction accuracy. Colonoscopy is the gold standard approach for CRC screening [2] and implementing population-based CRC screening programs is an effective way to lower the incidence and mortality of CRC [3]. The purpose of these screening programs is to find and remove adenomatous polyps that may eventually lead to CRC [4]. Additionally, it is known that an early CRC diagnosis can raise the 5-year survival percentage from 18 to 88.5% [5]. Therefore, the screening and treatment of colorectal cancer are an urgent requirement. Many image processing techniques are finding their way into medical image analysis as digital technology advances and the usage of imaging improves dramatically in healthcare and diagnostics. Researchers worldwide are putting massive efforts into enhancing automated diagnosis systems, making it one of the most active research areas. The fundamental reason behind making (CAD) based systems widely accessible and useful involves medical image segmentation as it has been used as a popular image processing technique to ease and automate medical imaging tasks. During medical segmentation, the main objective is to extract the specific region of interest (ROI) from the medical images based on the intended application.

Accurate segmentation of rectal cancer and rectal wall is the primary task to guide the staging of rectal cancer and determine a suitable treatment plan. For several reasons, the segmentation of medical images is challenging. The images are captured under various different protocols and settings, so they have low contrast and are non-homogeneous in appearance, leading to problems like under-segmentation [6] or over-segmentation. There is a significant variation in

[1] *Research scholar, Department of CSE, Presidency University, Bangalore Email: prashanthphdcse@gmail.com*
[2] *Professor, Department of CSE, Presidency University, Bangalore Email: harisen1234@yahoo.co.in*
* *Corresponding Author Email: prashanthphdcse@gmail.com*

the scale and shape of images [7-8], due to which we can't construct a prior shape model. The various types of polyps, including large, small isochromatic, and diminutive polyps are shown in Figure 1.

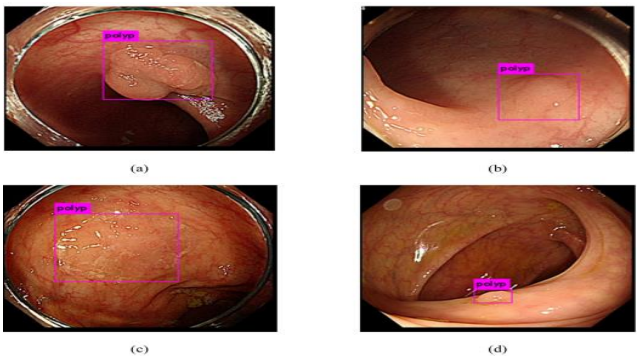

Fig 1. Examples of polyp detection in still-image analysis (dataset A). (a) Polypoid polyps, (b,c) isochromatic fat polyps, and (d) distant, diminutive polyp.

Early detection of polyps diseases is vital., Convolutional Neural Networks (CNNs) and Vision Transformers (ViTs) have emerged as effective tools for medical image analysis with the advent of deep learning. These technologies have shown exceptional performance in a variety of diagnostic tasks. Using a Cascade CNN-ViT model, which blends the capabilities of Inception-V3, ResNet-50, and Vision Transformer architectures, we suggest a novel method in this study to detect the polyps. This method makes use of a Cascade CNN-ViT model. Each of these components adds its own unique set of characteristics and advantages, which enables improved illness categorization based on ~~retinal~~ image features and more accurate feature representation [14]. It has been demonstrated that convolutional neural networks (CNNs), such as Inception-V3 and ResNet-50, are very adept at learning hierarchical representations of images from their inputs. Inception-V3 makes use of inception modules to capture multi-scale features, whilst ResNet-50 implements skip connections as a solution to problems with disappearing gradients[29-30].

These architectures are particularly effective at extracting local and spatial features, which are necessary for determining abnormalities and detailed structures present in colonoscopy images. On the other hand, have attracted a lot of attention because of their capacity to incorporate self-attention processes. This ability enables the model to capture global contextual information as well as long-range relationships inside the image. ViTs are able to gain a more comprehensive grasp of the colonoscopy images as a result of this because they are able to learn the relationships between the various image regions and consider the interactions that occur between the various anatomical structures in the colonoscopy images. A Cascade CNN-ViT model has been presented, with the goal of improving the performance of polyps detection. This model takes advantage of the complementing qualities of both CNNs and Vision Transformers. By feeding the local features derived by Inception-V3 and ResNet-50 into the Vision Transformer, the model is able to successfully combine fine-grained local information with a semantically relevant global context. As a result, the model has better discriminative power when it comes to disease categorization[14].

In addition, the Cascade CNN-ViT model that was developed demonstrates the broader potential of synergistic integration of deep learning architectures for increasing medical image analysis, particularly in difficult and high-dimensional medical datasets. This was accomplished by using the model. Retinal illnesses, Cascade CNN-ViT, Inception-V3, ResNet-50, Vision Transformer, Deep learning, Medical image analysis, Early diagnosis, Multimodal retinal imaging, and Vision Transformer are some of the keywords that have been associated with this topic. The paper is structured as follows: Section 2 reviews related work. Section 3 describes the main steps of the research methodology. In Section 4, the dataset is described and ablation experiments are performed to evaluate performance metrics, demonstrate the working principle of the Polyp method, and provide directions for future research. Section 5 concludes the paper.

2. Related Works

Polyps are an essential sign of early colon cancer, so the main purpose of the examination is to detect them as early as possible to improve patient survival rates. Automatic detection and localization of polyps in video frames of gastrointestinal endoscopy can help reduce missed and false detections in manual manipulation, improve detection quality and efficiency, and have positive implications for the early detection of pre-cancerous lesions.

Later, some researchers developed an interest in learning the temporal relationship among the images. For segmenting the ROI from the medical images, they used recurrent neural networks (RNNs) to predict the temporal dependency among the image sequences. In this field, researchers have integrated RNNs with different architectures to improve performance. Gao et al. [9] enhanced segmentation accuracy by integrating CNN and LSTM to learn the time-dependent relationship between different images. To obtain spatiotemporal information, Bai et al. [10] used RNN and FCN for aortic sequence segmentation. The RNNs are generally employed to determine the image's global and local spatial features when the context is considered. Despite the potential benefits of using RNNs in medical image segmentation, it is still challenging to capture accurate and comprehensive temporal information. The primary reason why RNN architectures struggle to effectively address medical image segmentation is the limited availability and poor quality of medical image data[17-18].

In 2020, Dharmarajan et al. [11] recommended a machine-learning approach for the prediction of polyps using colonoscopy images. In this, the decision tree attribute splitting rule has been demonstrated to classify the thyroid nodules very efficiently and accurately. The diagnosis of thyroid disease was done with the help of machine learning classifiers like Naïve Bayes, regression techniques, neural networks, decision trees, and Support Vector Machine (SVM). The classification accuracy of the developed model was higher when analysed through the prior models.

Ronneberger et al.[16] designed U-Net for biomedical images. Owing to its excellent performance, U-Net and its variants have been widely used in various subfields of computer vision and image processing.–Seung-Hwan Bae and Kuk-Jin Yoon (2018)[20] employed a partial least squares (PLS) approach to find polyps in 1263 private pictures and the CVC ColonDB. The technique's objective was to build an impartial detector out of an uneven database. An improved identification method called discriminative feature learning was employed since the appearance of polyp and non-polyp patches is comparable. The suggested system was tested on CVC ColonDB and yielded precision, recall, F1, and F2 scores of 70.67%, 70.67%, and 70.67%, respectively. For the purpose of differentiating between polyps and healthy tissue, Wang et al. (2020)[21] used two straightforward features based on a co-occurrence matrix and a colour texture feature. Images of polyps and normal tissue were categorized using the SVM classifier. Seventy-four colonoscopic images were used in the investigation, which yielded a sensitivity of 86.2% and an FP rate of 1.26 marks per image.

For the categorization of colonic polyps, Wei Wang et al. (2020)[22] developed a deep learning technique using Global Average Pooling (GAP) in two pre-trained models. They conducted tests on the 1000 polyp and 7000 non-polyp photos in the CP-CHILD-A dataset, and both models had an accuracy of 98%. Jorge et al. (2017)[23] conducted a comparison of various Convolutional Neural Networks (CNN) for polyp identification and hybrid techniques. They discovered that the CUMED, CNN-based technique performed well for polyp detection. The ETIS-Larib database was used to assess the suggested CNN, and the results showed that it had a precision value of 72.36%, a recall value of 69.23%, an F1-score of 70.76%, and an F2-score of 69.83%.

Two feature improvement modules were introduced to the detector to aid in learning more about the features, and Sudhir et al. (2019)[19] 2-D CNN technique was utilized to identify the polyp in the static images. A transfer learning module was included to increase the sensitivity of polyps. The detector's data were integrated and the decision was made using a correction unit based on the inter-frame similarity assessment. Four databases—CVC-ClinicDB, ETIS-Lirib, CVC-ClinicDB, and RenjiVideoDB—were used to assess the suggested method. On the ETIS-Larib dataset, the 2D CNN models generated precision values of 83.24%, recall values of 71.63%, F1-scores of 77.00%, and F2-scores of 73.69%.

3. Methodology

3.1. PRE-PROCESSING

Colonoscopy images of different patients have different dimensions. Therefore, in the first stage of preprocessing, the dimensions of all images are changed to 320×320. Then a new hybrid color space is created from the RGB and H×S×V color spaces. The lightness component is not separated from the color components in RGB color space. Therefore, the images are transferred from the RGB space to the H×S×V space. Because the polyp tissue is similar to the normal colon tissue, the lightness channel of the H×S×V color space replaces the red channel. As a result, the HSV color space will be created. According to Figure 2, it can be expected that the sharpness of the polyp edges will increase in the proposed hybrid color space.

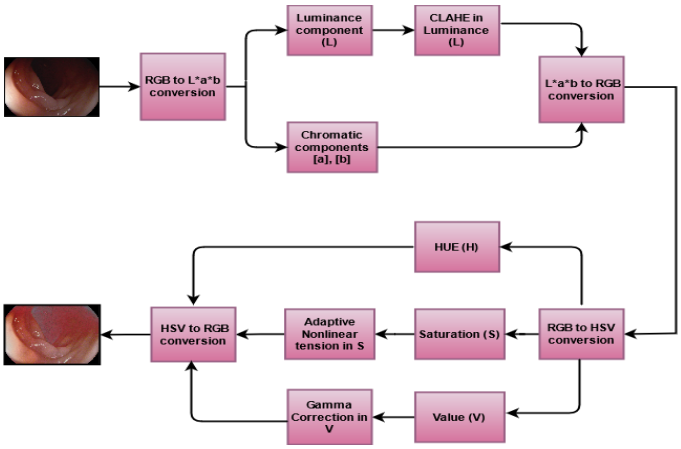

Fig. 2. The pre-processing stage of RGB to HSV conversion.

3.2 FCGAN for poly segmentation

The Full Convolution Generate Network (FCGN) model is used to predict the segmentation image, which is then fed to the discriminant convolutional network for training together with the real labeled segmented image. The goal of the proposed method is to make accurate discrimination between the Discriminant Convolutional Network (DCN) and FGN impossible. To optimize the generator's performance and to improve the accuracy of the segmentation, through adversarial mutual learning between the generator and discriminator. Two improved approaches based on the generation adversarial network are performed: 1) Instead of using a convolutional network as a generated model, utilize a full convolutional generate network and pixel-level semantic classification instead of image-level semantic classification to create end-to-end segmentation results and speed up segmentation

computations. 2) Directly utilize the segmentation output from the FGN and the real label input to DCN for more comprehensive classification.

3.2.1 Full Convolution Generate Network.

A fully convolutional network model as a generator. This network structure combines the advantages of FCN and U-Net to reduce the size of the U-Net in terms of network depth, reduce the loss of low-level semantic information, and result in end-to-end image polyps segmentation. Figure 3 depicts the model structure. The network structure is made up of seven hidden layers, with the feature compression path and the recovery restoration path being the most important. The feature compression approach uses the max-pooling operation and contains three convolutional layer groups, each followed by a downsampling layer. The intermediate feature map is obtained using a layer of 33% convolution in the fourth layer. The feature extraction pipeline consists of three upsampling layers. The 1x1 and softmax activation functions are used to translate multi-channel features into relevant categories in the final set of convolutional layers. Each of the six groups of convolutional layers in the compression and feature restoration paths consists of two sets of convolution operations, and convolutions from the same cluster of convolutional layers have the same convolution kernel parameters, including batch processing and activation functions. As in the case of the U-Net network, the feature recovery path will merge the output of the feature extraction portion across the skip connection, resulting in an upsampled feature map that not only has deep high-level semantic information but also has rich low-level semantic information to improve segmentation accuracy.

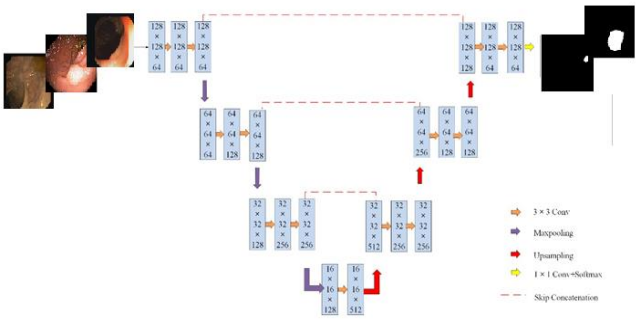

Fig.3. The structure diagram of the FGN

The semantic information loss of the fully convolutional network is one element of the loss function of the FGN, while the adversarial loss created by the GAN is the other. Note that the challenge of poly segmentation has a severe category imbalance. Normal tissue or black backdrop accounts for 98.46% of the area, 1.02% of the edema region, 0.29% of the enhancing tumor, and a minimum of 0.23% of the necrotic and non-enhanced occupied region[32]. For better task prediction and estimation, this paper uses the combined weighted cross entropy (WCE) [33] and the generalized dice loss (GDL)[31] for semantic information loss and the binary cross entropy loss to combat the loss. Therefore, the definition of the combined loss function is as follows,

$$Loss = L_{WCE} + L_{GDL} + L_{CE} \tag{2}$$

Weighted cross entropy (WCE) is a cross-entropy loss modification in which all positive samples are multiplied by a weighting coefficient to tackle the problem of category imbalance and mitigate the disparity between training samples and assessment metrics. The loss function generalized dice (GDL) is often utilized in medical image segmentation. When there are numerous locations in a lesion (such as polys), each category will have a dice (DICE), and the GDL will combine the DICE of multiple classes, allowing the model to focus on the difficult-to-learn samples. However, when GDL is working with very unbalanced data, training stability is not assured. GDL is responsible for predicting the segmentation area, and WCE is used for the classification of tissue cells. This mixed-loss function can lift the gradient of difficult-to-classify data while decreasing the gradient of easy-to-classify samples, which may partially mitigate the problem of category imbalance in poly segmentation. The calculation formula for these two parameters is,

$$L_{GDL} = 1 - \frac{2\sum_{i}^{I} w_i k_i p_i}{\sum_{i}^{I} w_i \left(k_i + p_i\right)} \tag{3}$$

$$L_{WCE} = -\sum_{i}^{I} w_i k_i \log\left(p_i\right) \tag{4}$$

where I is the total number of labels, which w_i means the weight assigned to the i-th label. p_i and k_i denote the pixel value of the segmented binary image and the binary ground truth image, respectively. L_{CE} represents the adversarial loss function generated by the DCN, and the calculation formula is given in Equ. (5). The DCN generates the loss function, which is used to decide if the source is valid, and the error is fed back to the Full Convolution Generate network, allowing the segmentation model to attain better accuracy.

$$L_{CE} = -\left(y \log\left(D\left(G_{inputs}\right)\right) + \left(1 - y\right) \log\left(1 - D\left(G_{inputs}\right)\right)\right) \tag{5}$$

Where y belongs to $(0,1)$ is the label value, $D(G(X_{inputs}))$ is the probability that the discriminator predicts the generator to predict that the sample is a positive number.

3.3.2 Discriminant Convolutional Network(DCN)

DCN uses CNN to evaluate whether the input data is true or false. The genuine segmentation result is given a label of

1, whereas the anticipated segmentation result is given a label of 0. The model structure is shown in Figure 4,

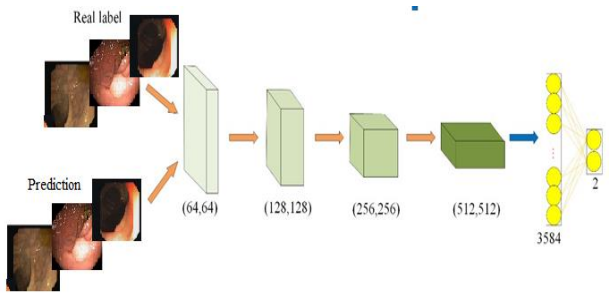

Fig.4. The structure diagram of the DCN

The DCN consists of six layers, each of which is divided into two parts: the first four convolutional layers for feature extraction and the second two fully connected layers for decreasing the influence of feature location. Each of the first four convolutional layer groups has two convolutions with the same convolution kernel size, with 64, 128, 256, and 512 convolution kernels, respectively. The convolution group's step size of convolution is set to 2 in order to perform the down-sampling process. To give the model greater nonlinear capabilities, the first four convolutional layers employ LeakyRelu as the activation function. The fifth and sixth layers are fully connected layers with a sigmoid activation function to obtain probability values for real labeled samples and anticipated segmentation result images. The binary cross-entropy as the loss function of the DCN, is still used to measure the error between the real result and the predicted result, the larger the error, the poorer the segmentation model, and conversely the smaller the error the higher the accuracy of the model segmentation, as defined by Equ.6.

$$L_D = -\log\left(D_{labels}\right) - \log\left(1 - D\left(G_{inputs}\right)\right) \quad (6)$$

Where L_D is the loss function of the DCN, $D(\,)$ is the classification result of the DCN, and $G(\,)$ is the predicted segmentation result.

4. Data Set Description and Performance Measures

4.1. Dataset Description

The experiment was performed using publicly available databases such as ETIS-Larib [25], this dataset contains 196 polyp images. The second Dataset CVC-ClinicVideoDB [26] consists of 11,954 images in total with 10,025 images of polyp. The third Data set Kvasir-SEG [27] consists of 1000 polyp images. Colonoscopy images of 592 subjects are randomly divided into a training set of 572 cases and a test set of 65 subjects, , which are completely separated from the training set. Data augmentation includes random horizontal flip and random vertical filp. The performance of the method is evaluated by performing multi-class segmentation (i.e., segmenting rectal cancer and rectal wall) and calculating the DSC, specificity, and sensitivity of the targets in the segmentation map and the objects in the manual annotation results.

4.2. Performance Measures

In this study, three widely adopted metrics are used to evaluate the final segmentation results: dice similarity coefficient (DSC), specificity (Spec.) and sensitivity (Sen.).It is given in the following eqns.

$$\mathrm{Se} = \frac{TP}{TP+FN}$$

$$\mathrm{Pr} = \frac{TP}{TP+FP}$$

$$\mathrm{Sp} = \frac{TN}{TN+FP}$$

$$\mathrm{ACC} = \frac{TP+TN}{TP+FP+TN+FN}$$

$$\mathrm{F_1} = 2 \cdot \frac{\mathrm{Se} \cdot \mathrm{Pr}}{\mathrm{Se} + \mathrm{Pr}}$$

5. Results and Discussion

5.1. PERFORMANCE OF PROPOSED FCGN METHOD

To better verify the advantages of the proposed FCGN on polyp segmentation, quantitative and qualitative analyses are introduced for experiment analysis, and detailed experiments are carried out on these three public datasets. The comparison experiment is first carried out for each dataset and advanced segmentation models to demonstrate the superiority of the proposed FCGN on polyp segmentation. Second, ablation research is also carried out to demonstrate the viability of each network block that has been proposed. To compare intuitive performance, the visualization experiment is also run on the experiment datasets. The specific experiment details and results are given as follows.

5.1.1. Performance on Kvasir-SEG Dataset

To demonstrate the superior performance of the proposed FCGN, a comparative experiment is conducted in this paper. Here, some segmentation models performed in the Kvasir-SEG dataset in recent years served as comparison networks, including CNN-based methods such as U-Net, Deeplabv3+,UNet++,CE-Net and Inf-Net. The experimental results of FCGN on **Kvasir-SEG dataset is given in Table 1.**

Table 1 Experimental results of FCGN and Other models on the Kvasir-SEG dataset

Method	IoU	DSC	Acc	Se	Sp	Pr
U-Net++[18]	94.24	97.21	97.89	97.44	98.51	97.11
DeepLabv3+[28]	93.23	95.28	97.42	96.19	97.67	96.89
ECA-net[21]	92.53	96.88	97.12	97.29	97.67	96.89
UNet [16]	92.23	97.88	96.98	96.19	97.67	96.89
Ce-Net [17]	90.11	94.22	92.34	92.21	92.23	92.21
Inf-Net[19]	91.61	95.12	91.89	90.12	92.11	92.23
FCGN	**97.34**	**98.74**	**98.34**	**98.63**	**98.23**	**97.89**

5.1.2. PERFORMANCE ON CVC-ClinicVideoDB DATASET

The performance of the FCGN Net on the CVC-ClinicVideoDB data set is given in Table 3. It can be concluded from Table 2 that, when employing the same model, the segmentation performance of the CVC-ClinicVideoDB dataset is marginally worse to that of the Kvasir-SEG dataset. The U-Net has the greatest specificity and precision metrics values, at 97.11 and 94.21, respectively.

Table 2 Experimental results of FCGN and Other models on the CVC-ClinicVideoDB dataset.

Method	IoU	DSC	Acc	Se	Sp	Pr
U-Net++[18]	92.23	96.88	97.12	96.19	97.67	96.89
DeepLabv3+[28]	90.98	93.98	96.84	96.13	97.17	94.21
ECA-net[21]	85.99	92.81	97.12	96.89	97.34	89.26
UNet [16]	90.98	93.98	96.84	96.13	97.17	94.21
Ce-Net [17]	94.14	97.21	97.89	97.11	98.51	97.11
Inf-Net[19]	91.61	95.12	91.89	90.12	92.11	92.23
FCGN	**96.23**	**97.67**	**98.34**	**98.78**	**98.45**	**96.89**

5.1.3. PERFORMANCE ON ETIS-Larib DATASET

ETIS-Larib Data set has a limited number of images with varying resolutions. Every image was scaled down to 256 256 while preserving its aspect ratio. By flipping and mirroring the photos, the training set's original 400 images were increased to 500. Table 3 provides a summary of the performance comparisons. Figures 5 and 6 show the results of polyp segmentation using a different approach and a 0.5 IoU threshold for Kvasir-SEG and ETIS-Larib, respectively.

Table 3 Experimental results of FCGN and Other models on the ETIS-Larib dataset.

Method	IoU	DSC	Acc	Se	Sp	Pr
U-Net++[18]	92.53	96.88	97.12	97.29	97.67	96.89
DeepLabv3+[28]	95.23	97.88	96.98	96.19	94.61	95.67
ECA-net[21]	86.11	91.13	93.33	95.34	95.34	88.54
UNet [16]	92.53	96.88	97.12	97.29	97.67	96.89
Ce-Net [17]	85.99	92.81	97.12	96.89	97.34	89.26
Inf-Net[19]	94.14	97.21	97.89	97.11	98.51	97.11
FCGN	**97.98**	**96.98**	**97.84**	**98.13**	**98.17**	**97.21**

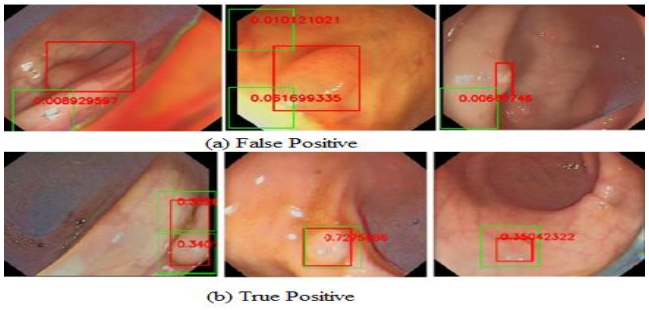

Fig 5: Experimental results of the proposed method on Kvasir-SEG Dataset

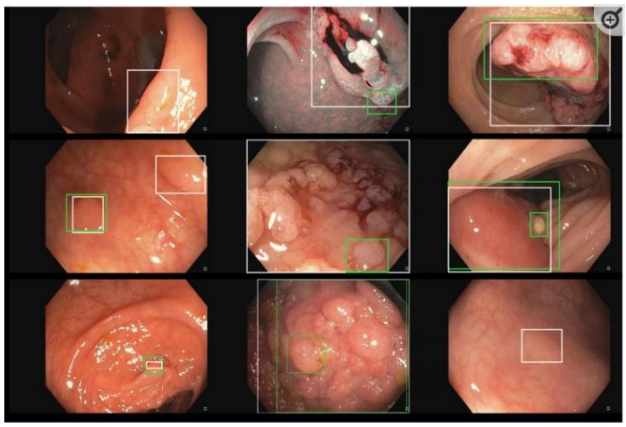

Fig 6: Experimental results of the proposed method on ETIS-Larib DATASET, the segmentation part of the proposed method is marked in Green, and the Ground truth is marked in white.

6. Conclusion

This work proposes an efficient architecture based on FCG-Net with improved and efficient performance. Unlike previously proposed variants of fully conventional Generator models, the proposed model gives promising results in segmenting the given medical image by effectively reducing the over-fitting and computational requirements. It can also input the segmentation prediction images and the labeled images into the discriminant convolutional network and improve the segmentation accuracy of CRC by further enhancing the essential characteristics of learning data through the confrontation training of generators and discriminators. FCG-Net can also input the segmentation prediction images and the labeled images into the discriminant convolutional network and improve the segmentation accuracy of polyps by further enhancing the essential characteristics of learning data through the confrontation training of generators and discriminators. In conclusion, the choice of a deep learning model depends on several factors, and it is not always necessary to use the deepest model to achieve the best performance on a specific task. It is important to evaluate different models and select the one that best suits the specific needs of the project.

Conflicts of interest

The authors declare no conflicts of interest.

References

[1] Bai, W., Suzuki, H., Qin, C., Tarroni, G., Oktay, O., Matthews, P.M., Rueckert, D.: Recurrent neural networks for aortic image sequence segmentation with sparse annotations. In: International Conference on Medical Image Computing and Computer-assisted Intervention, pp. 586–594 (2018). Springer

[2] US Preventive Services Task Force, Bibbins-Domingo K, Grossman DC, Curry SJ, Davidson KW, Epling JW, García FAR, Gillman MW, Harper DM, Kemper AR, Krist AH, Kurth AE, Landefeld CS, Mangione CM, Owens DK, Phillips WR, Phipps MG, Pignone MP, Siu AL (2016) Screening for colorectal cancer: US preventive services task force recommendation statement. JAMA 315:2564. https://doi.org/10.1001/jama.2016.5989.

[3] Cubiella J, González A, Almazán R, Rodríguez-Camacho E, Zubizarreta R, Peña-Rey Lorenzo I (2020) Overtreatment in nonmalignant lesions detected in a colorectal cancer screening program: a cross-sectional analysis. Res Sq. https://doi.org/10.21203/rs.3.rs-113901/v1

[4] Zauber AG, Winawer SJ, O'Brien MJ, Lansdorp-Vogelaar I, van Ballegooijen M, Hankey BF, Shi W, Bond JH, Schapiro M, Panish JF, Stewart ET, Waye JD (2012) Colonoscopic polypectomy and long-term prevention of colorectal-cancer deaths. N Engl J Med 366:687–696. https://doi.org/10.1056/NEJMoa1100370

[5] Wiegering A, Ackermann S, Riegel J, Dietz UA, Götze O, Germer C-T, Klein I (2016) Improved survival of patients with colon cancer detected by screening colonoscopy. Int J Colorectal Dis 31:1039–1045. https://doi.org/10.1007/s00384-015-2501-6

[6] Jayachandran, A and R.Dhanasekaran ,(2017) 'Multi Class Brain Tumor Classification of MRI Images using Hybrid Structure Descriptor and Fuzzy Logic Based RBF Kernel SVM' , Iranian Journal of Fuzzy system , Volume 14, Issue 3, pp 41-54 , 2017.

[7] Mahiba C, A Jayachandran,"Severity analysis of diabetic retinopathy in retinal images using hybrid structure descriptor and modified CNNs",Measurement,Vol 135,PP 762-767,2019.

[8] Jayachandran, A, 'Abnormality segmentation and Classification of multi model brain tumor in MR images using Fuzzy based hybrid kernel SVM' International Journal of Fuzzy system , published by Springer, Volume 17, Issue 3, pp 434-443,2018.

[9] Gao, Y., Phillips, J.M., Zheng, Y., Min, R., Fletcher, P.T., Gerig, G.: Fully convolutional structured lstm networks for joint 4d medical image segmentation. In: 2018 IEEE 15th International Symposium on Biomedical Imaging (ISBI 2018), pp. 1104–1108 (2018). IEEE

[10] Jayachandran, A & Dhanasekaran, R, "Severity Analysis of Brain Tumor in MRI Images using Modified Multi-Texton Structure Descriptor and Kernel- SVM, The Arabian Journal of science and engineering October 2014, Volume 39, Issue 10, pp 7073-7086,(2014).

[11] K. Dharmarajan, K. Balasree, A.S. Arunachalam, K. Abirmai, "Polyps Disease Classification Using Decision Tree and SVM," Indian Journal of Public Health Research & Development, vol. 11, No. 03, March 2020.

[12] Haque IRI, Neubert J. Deep learning approaches to biomedical image segmentation. Informatics in Medicine Unlocked. 2020;18:100297.

[13] Jayachandran, DS David,"Textures and intensity histogram based retinal image classification system using hybrid colour structure descriptor",Biomedical and Pharmacology Journal,PP 577-582,Vol 11,issue 1,2018.

[14] "EfficientNet: Rethinking Model Scaling for Convolutional Neural Networks" - Tan M. et al. (2019) [Link:

[15] "Deep learning-based segmentation of pathologic complete response on rectal MRI after neoadjuvant therapy: A multicenter study" - Kim JH. et al. (2018) [Link: https://doi.org/10.1016/j.radonc.2018.08.022].

[16] Ronneberger, O., Fischer, P., Brox, T.: U-net: Convolutional networks for biomedical image segmentation. In: International Conference on Medical Image Computing and Computer-assisted Intervention, pp. 234–241

[17] Gu, Z., Cheng, J., Fu, H., Zhou, K., Hao, H., Zhao, Y., Zhang, T., Gao, S., Liu, J.: Ce-net: Context encoder network for 2d medical image segmentation. IEEE transactions on medical imaging 38(10), 2281–2292 (2019).

[18] Zhou, Z., Siddiquee, M.M.R., Tajbakhsh, N., Liang, J.: Unet++: Redesigning skip connections to exploit multiscale features in image segmentation. IEEE Transactions on Medical Imaging 39(6), 1856–1867 (2020).

[19] Fan, D.-P., Zhou, T., Ji, G.-P., Zhou, Y., Chen, G., Fu, H., Shen, J., Shao, L.: Inf-net: Automatic covid-19 lung infection segmentation from ct images. IEEE Transactions on Medical Imaging 39(8), 2626–2637 (2020)

[20] Seung-Hwan Bae and Kuk-Jin Yoon. Polyp detection via imbalanced learning and discriminative feature learning. IEEE transactions on medical imaging, 34(11):2379–2393, 2018.

[21] Wang, B. Wu, P. Zhu, P. Li, W. Zuo, and Q. Hu, "ECA-Net: Efficient Channel Attention for Deep Convolutional Neural Networks," in Proc. IEEE Conf. Comput. Vis. Pattern Recognit., pp. 11531–11539, 2020.

[22] Wei Wang, Jinge Tian, Chengwen Zhang, Yanhong Luo, Xin Wang, and Ji Li. An improved deep learning approach and its applications on colonic polyp images detection. BMC Medical Imaging, 20(1):1–14, 2020.

[23] Jorge B, Nima Tajkbaksh, Francisco Javier S´anchez, Bogdan J Ma- tuszewski, Hao Chen, Lequan Yu, Quentin Angermann, Olivier Romain, Bjørn Rustad, Ilangko Balasingham, et al. Comparative validation of polyp detection methods in video colonoscopy: results from the miccai 2015 endo-scopic vision challenge. IEEE transactions on medical imaging, 36(6):1231– 1249, 2017.

[24] Sudhir S, Frank Meng, and Steven Yi. Region-based automated localization of colonoscopy and wireless capsule endoscopy polyps. Applied Sciences, 9(12):2404, 2019.

[25] Silva J.S., Histace A., Romain O., Dray X., Granado B. Toward embedded detection of polyps in WCE images for early diagnosis of colorectal cancer. Int. J. Comput. Assist. Radiol. Surg. 2013;9:283–293.

[26] Bernal J.J., Histace A., Masana M., Angermann Q., Sánchez-Montes C., Rodriguez C., Hammami M., Garcia-Rodriguez A., Córdova H., Romain O., et al. Polyp Detection Benchmark in Colonoscopy Videos using GTCreator: A Novel Fully Configurable Tool for Easy and Fast Annotation of Image Databases; Proceedings of the 32nd CARS Conference; Berlin, Germany. 22–23 June 2018. [Google Scholar]

[27] Jha D., Smedsrud P.H., Riegler M.A., Halvorsen P., de Lange T., Johansen D., Johansen H.D. Kvasir-SEG: A Segmented Polyp Dataset. Int. Conf. Multimed. Model. 2019;11962:451–462. doi: 10.1007/978-3-030-37734-2_37.

[28] Yang Z, X. Peng, and Z. Yin, "Deeplab v3 plus-net for image semantic segmentation with channel compression," in Proceedings of IEEE 20th International Conference on Communication Technology (ICCT). IEEE, 2020, pp. 1320–1324.

[29] Jesu Prabhu A and Jayachandran, A, "Mixture Model

Segmentation System for Parasagittal Meningioma Brain Tumor Classification based on Hybrid Feature Vector" Journal of Medical System, vol 42, issues 12, 2018.

[30] Jha D, Smedsrud PH, Riegler MA, Johansen D, De Lange T, Halvorsen P, et al., editors. Resunet++: An advanced architecture for medical image segmentation. 2019 IEEE International Symposium on Multimedia (ISM); 2019: IEEE.